# INVESTIGATION ON VARIABLE-HEIGHT PROTRUSION ARRANGEMENT OF METAL-COMPOSITE HYBRID JOINTS UNDER A TENSILE LOAD

Yueran Zhao<sup>1</sup>, Wenzhi Wang<sup>1</sup>, Xiaopeng Wan<sup>1</sup>

<sup>1</sup> School of Aeronautics, Northwestern Polytechnical University, Xi'an, P.R. China

#### **Abstract**

Metal—composite hybrid joining with protrusion reinforcement is considered an effective way to improve the joint efficiency of aeronautical structures. Based on the failure process of hybrid joints obtained from previous research, this study investigated the influence of protrusion arrangement on joint performance by altering the protrusion height. A series of single lap joints with variable-height protrusions were designed and modeled using the finite element method. Numerical investigation was conducted to analyze the stress distribution and failure behavior of these hybrid joints. The results showed that the stress concentration region of joints was located in different positions, and the reinforcing efficiency of metal protrusions varied across the metal—composite interface. Protrusions near the metal and composite ends have a greater impact on loading capacity than protrusions in the middle of overlapping area. It is suggested that a hybrid joint with high metal protrusions at the edge and low protrusions in the center can suppress delamination failure without losing strength. These findings provide guidance for optimal protrusion array design to achieve better hybrid joining performance.

Keywords: Composites; Metal-composite joints; Pin-reinforced joining; Failure analysis

#### 1. Introduction

With the widely application of advanced composite materials in the aerospace industry, connection between the composite and metal structures gradually becomes an inevitably issue. Considering the severe stress concentration of mechanical fastening and relatively weak load capacity of adhesive bonding [1], various innovative hybrid joining methods were developed in recent years, including through-the-thickness reinforced metal—composite joining. Integrated the advantages of mechanical fastening and adhesive bonding, hybrid joint with protrusion reinforced is proved to have higher structural strength and damage tolerance [2, 3].

The configuration of metal protrusions has a significant impact on the ultimate strength and failure behavior of hybrid joint, such as shape, dimension and density [4-7]. However, very few research were conducted on the influence of protrusion arrangement [8]. Due to the stiffness mismatch between metal and composite adherends, experiments designed by Graham et al [9] showed that the failure of composite occurred much earlier than expected and therefore used less protrusions around the edge. Xiong et al [6] indicated that the efficiency of the protrusions was different at the metal and composite ends of the overlapping area, the stress concentration of the composite end is greater than that of the metal end, and the residual protrusion heights after joint failure varied along the bond line. Based on our previous work and experimental observations [10], stress concentration can be clearly observed around the top of protrusions, and crack extended quickly between the composite layer when delamination first occurred. This enlighten us that a variable-height protrusion design may be able to suppress the interaction between stress fields around protrusion tip and slow down the delamination crack propagation.

In this work, eight hybrid joint models with various protrusion height distributions were designed and established in ABAQUS<sup>TM</sup>. To fully understand the load-bearing and damage mechanisms of variable-height pin-reinforced joints, the constitutive relationship of each material component, including failure criteria and damage evolution, were defined separately. The effectiveness of the

finite element model we built is verified by previous experimental data. Numerical analysis was then applied to investigate the stress distribution and failure behavior of these variable-height joints.

# 2. Methodology

# 2.1 Modeling methods

The structure of a representative pin-reinforced metal—composite single lap joint was illustrated in Figure 1. Typical trapezoidal configuration of single protrusion was applied for manufacturing convenience, and a staggered distribution of protrusion arrays was chosen to weaken the connection effect of stress fields between adjacent protrusions.

Three material components of hybrid joint, including metal, composite and interface, were built separately and then assembled together in ABAQUS<sup>TM</sup>. The metal and composite panel were modeled by 8-node linear brick elements (C3D8), while the interface component representing adhesive bonding was modeled by 8-node three-dimensional cohesive elements (COH3D8) with zero thickness. Cohesive elements were also inserted in composite layers to describe the delamination behavior of laminates. The lower and upper surface of interface elements were tied with metal and composite, respectively. During the loading procedure, the metal end was fixed in all direction, while a tensile displacement was exerted on the composite end. As a strong nonlinearity existed in this structural model, the Explicit solver was used to prevent convergence issue.

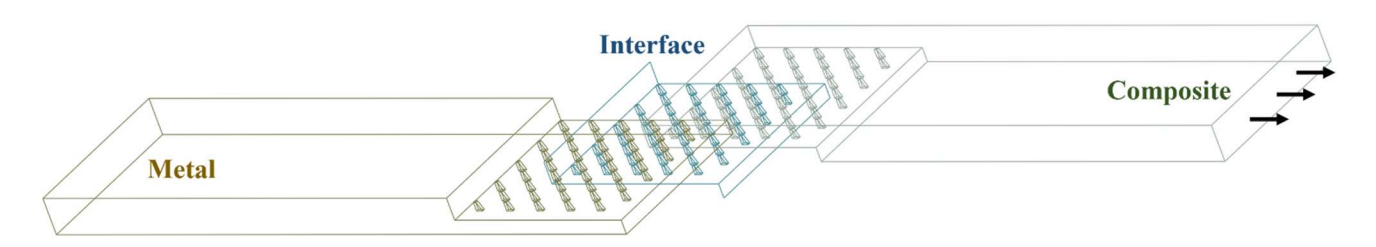


Figure 1 – Sketch of pin-reinforced metal–composite lap joint model.

To study the whole failure process of hybrid joints, the metal panel was defined as elastic-plastic material with ductile damage, and Hashin failure criteria were adopted to characterize the failure modes of composite. Bilinear softening law was used to describe the traction-separation behavior of cohesive zone model [11]. The constitutive relationships of composite and cohesive elements were introduced by user-defined material subroutine. For composite material, the Hashin failure criteria were given by [12]

(a) Fiber tensile failure:

$$\left(\frac{\sigma_{11}}{X_t}\right)^2 + \left(\frac{\sigma_{12}}{S_{12}}\right)^2 + \left(\frac{\sigma_{13}}{S_{13}}\right)^2 \ge 1 \tag{1}$$

(b) Fiber compression failure:

$$\left(\frac{\sigma_{11}}{\chi_c}\right)^2 \ge 1\tag{2}$$

(c) Matrix tensile failure:

$$\left(\frac{\sigma_{22} + \sigma_{33}}{Y_t}\right)^2 + \left(\frac{\sigma_{12}}{S_{12}}\right)^2 + \left(\frac{\sigma_{13}}{S_{13}}\right)^2 + \frac{\sigma_{23}^2 - \sigma_{22}\sigma_{33}}{S_{23}^2} \ge 1 \tag{3}$$

(d) Matrix compression failure:

$$\left[ \left( \frac{Y_c}{2S_{23}} \right)^2 - 1 \right] \frac{\sigma_{22} + \sigma_{33}}{Y_c} + \frac{(\sigma_{22} + \sigma_{33})^2}{4S_{23}^2} + \frac{\sigma_{23}^2 - \sigma_{22}\sigma_{33}}{S_{23}^2} + \left( \frac{\sigma_{12}}{S_{12}} \right)^2 + \left( \frac{\sigma_{13}}{S_{13}} \right)^2 \ge 1$$
 (4)

where  $X_t$ ,  $X_c$ ,  $Y_t$ , and  $Y_c$  are the longitudinal and transverse strength of laminates, respectively, and  $S_{12}$ ,  $S_{13}$ ,  $S_{23}$  are the shear strength on different composite plane.

Due to the complex failure modes of composite material, five damage variables were defined individually to express the extent of composite and cohesive failure. Characteristic length of element was applied in the calculation to reduce the mesh sensitivity of finite element model [13]. Considering the commonly used aeronautical structure materials, in our work, titanium alloy Ti-6Al-4V and carbon

fiber reinforced polymer T300/BA9916 were chosen for metal and composite materials. Mechanical properties of each component were adopted from previous research.

# 2.2 Design of variable-height protrusions

Based on our earlier investigation, the number of metal protrusions had great impact on loading capacity and fracture mode of pin-reinforced metal—composite joint. Hybrid joint with low protrusion density is hard to provide sufficient reinforcement for the metal—composite interface, while too many metal protrusions will cause excessive damage to composite panel and increase the structural weight. Therefore, in the current work, a medium protrusion number of hybrid joint was chosen to conduct further research. The protrusion array consists of 18 columns which was divided as odd and even column, respectively, as shown in Figure 2.

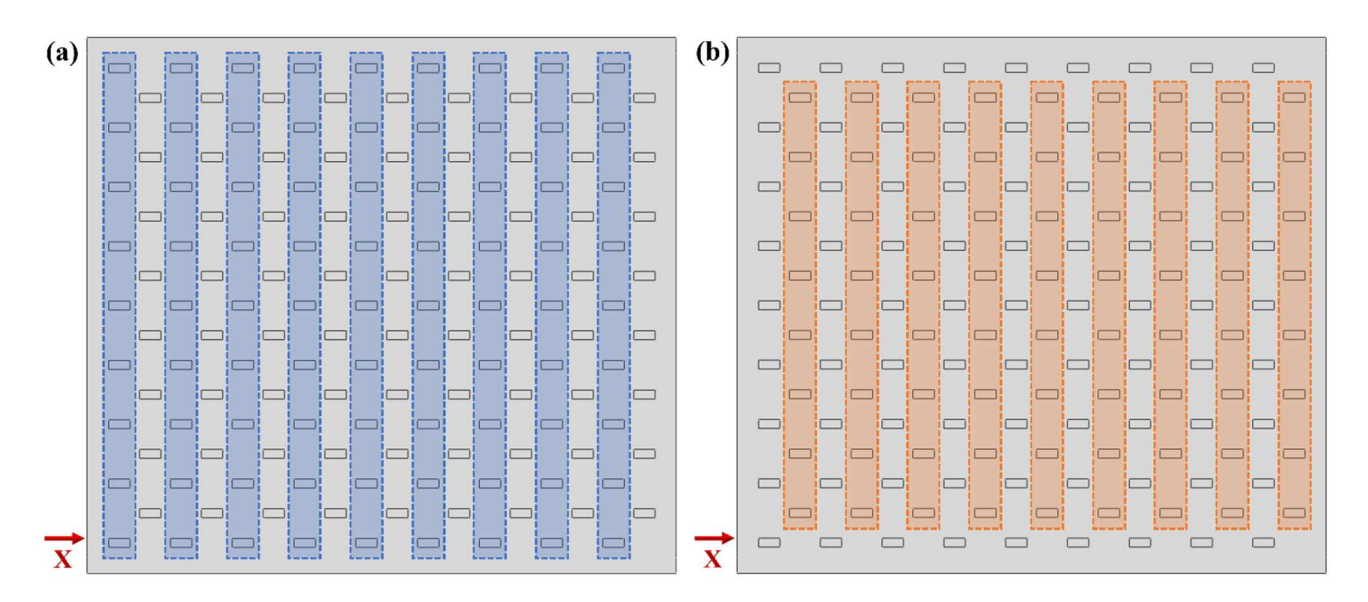


Figure 2 – Definition of (a) odd column and (b) even column of protrusions.

As the protrusion number and planar arrangement determined, the projection feature of variable-height hybrid joints was hold constant. In addition, the area of top and bottom surface of protrusions were all consistent, except for the shortest protrusion to avoid an excessive sharp angle. The only variable of eight joint models built in this work is the protrusion height in each column, and the sketch were drawn in Figure 3. To ensure that the influence of these inserted protrusions to laminate performance are similar, the total volume of metal protrusions was also carefully controlled.

First, three joint models with monotonically increasing, decreasing, and decrease-increasing protrusion height were established. In our model, the total thickness of composite panel in overlapping area is 3.92 mm, therefore, the intermediate value 1.96 mm was chosen as the base line of height. In these models, the highest protrusion is 3.64 mm, and the lowest protrusion is 0.28 mm. An additional joint model with constant height 1.96 mm was also constructed as reference, and its protrusion volume ratio is same with the other three models.

Then, inspired by the "wavy" configuration of single lap joint [14, 15], hybrid joints with sine and cosine height distribution were built to see the difference. Considering the single layer thickness of composite prepregs and taking integral multiples, the protrusion heights of these two variable-height joint models were approximately defined as

$$H = 1.68 + 1.4\cos(0.369(N-1)) \tag{1}$$

$$H = 1.68 + 1.4\sin(0.369(N + 11.8)) \tag{2}$$

where H is the protrusion height, N is the column of protrusion array in overlapping area, ranged from 1 to 18

Finally, left-eccentric and right-eccentric height distribution joint models were designed to investigate the influence of internal eccentric distribution. Due to the observations on previous model showed that an excessively low protrusion is of little use to joining performance, the lowest protrusion of these two eccentric joints was adjusted from 0.28 to 0.84 mm.

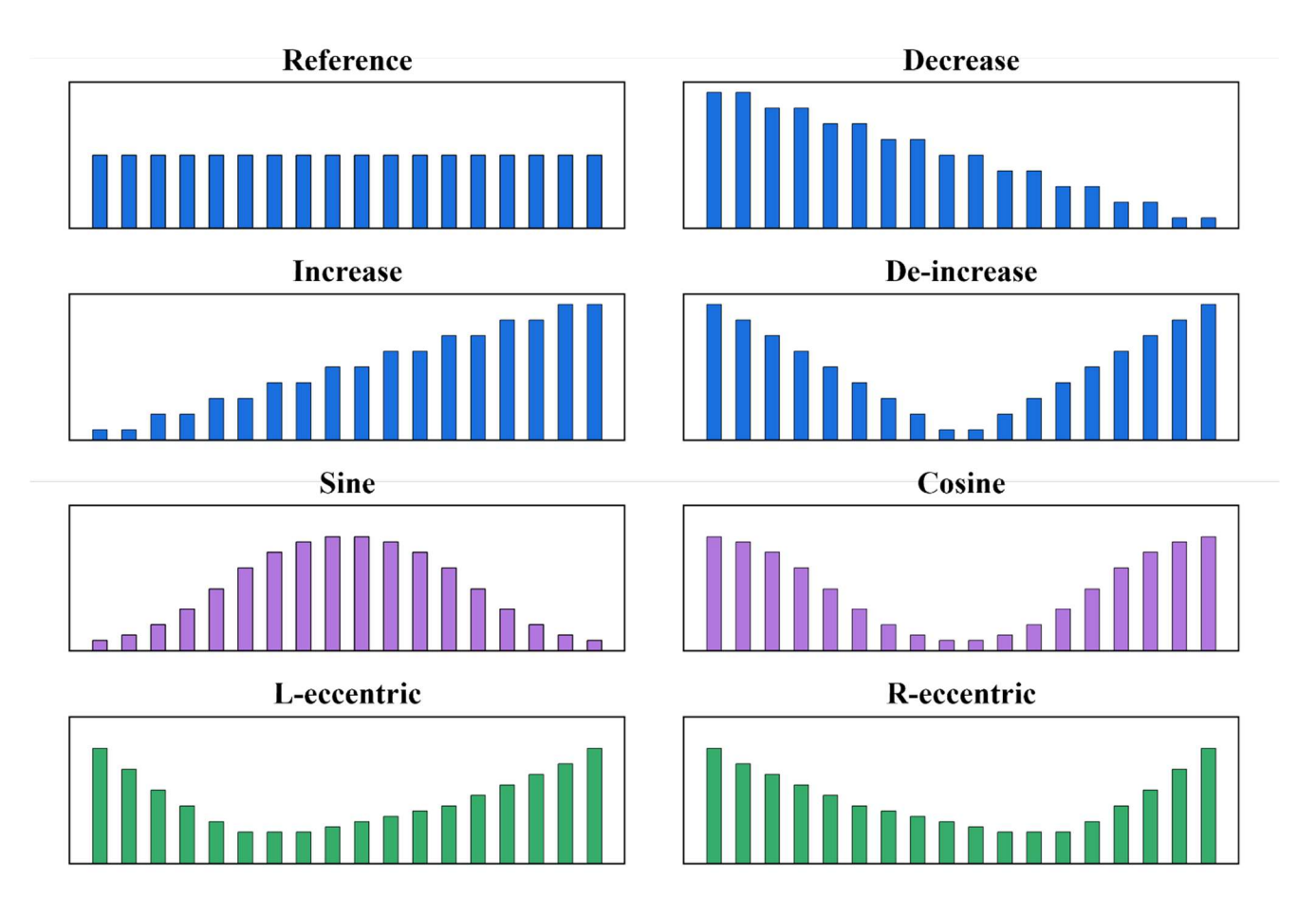


Figure 3 – Diagram of eight variable-height joint models.

# 3. Validation of numerical models

Combining the Selective Laser Melting technique of titanium alloy and co-curing method, different kinds of pin-reinforced metal—composite hybrid joint specimens were fabricated. Tensile tests were then conducted to calibrate the material properties applied in the numerical model [8]. The comparison on load—displacement curves and fracture morphology of joint models were given in Figure 4 and 5. The predicted strength and damage characteristic of all models showed good agreements with the experimental results. Although some deviation existed in the model with high protrusion density, which might be resulted from the manufacturing defects introduced by inserted protrusions, the failure process and damage mechanism were all rightly simulated. Therefore, the finite element modeling method built in our work can be used to conduct a quantitative analysis on the failure analysis of hybrid joint.

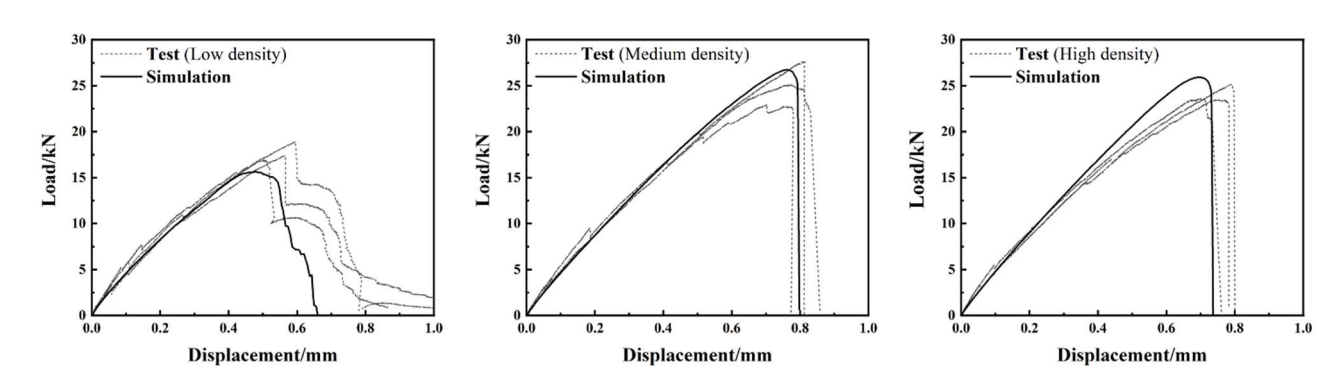


Figure 4 – Comparison on load–displacement curves of different models.

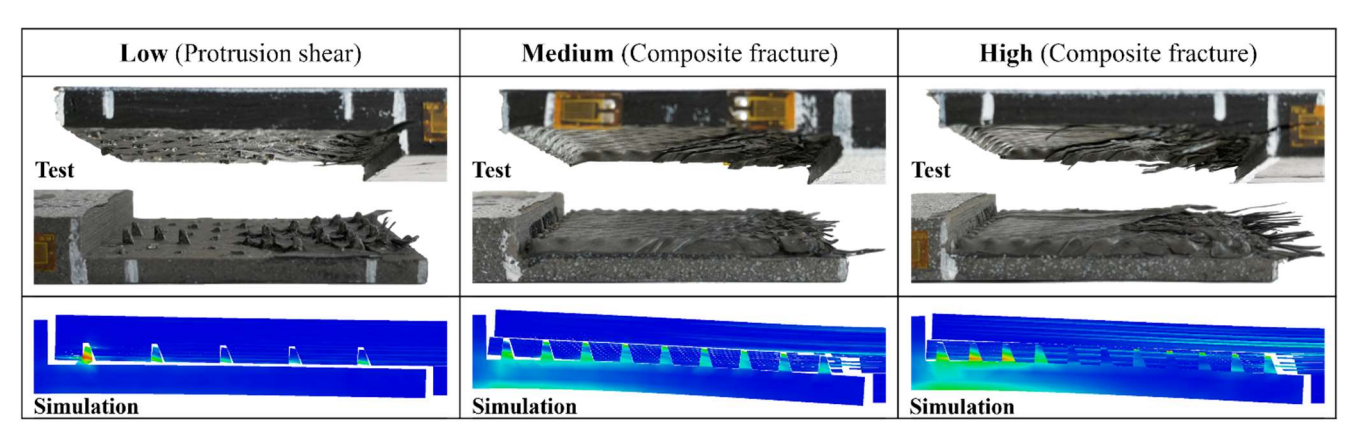


Figure 5 – Comparison on failure behavior of different models.

## 4. Results and discussion

# 4.1 Tensile performance of hybrid joints with variable-height protrusions

Figure 6 summarized the ultimate tensile load and displacement of different variable-height joint models. In the first group of joints, the single monotonically height design showed disadvantages in structural strength, especially for the decreasing height joint. This is because the reduced protrusion height weakens the loading capacity of edge. As the overlapping area nearing to composite ends is much critical than the metal ends, protrusions located in this region should be strengthened for better joint performance.

The maximum displacement in Figure 1 was defined as the tensile displacement when the joint structure reached its ultimate strength. It can be seen that the distribution of protrusion height has little effect on the maximum displacement. For example, although the ultimate strength of cosine joint model is 5.7% higher than that of the sine joint, the peak value occurred at the same tensile displacement, and the cosine height distribution resulted in higher structural stiffness. However, owing to the suppression of instantaneous delamination failure, joints with variable-height protrusions often exhibited better ductility after strength reached its maximum value.

For the two eccentric distributed joints studied in this work, their mechanical behavior is nearly consistent. This suggested that it is the peripheral protrusions controlled the ultimate strength, thus changing the internal protrusion height distribution had little effect on structural performance. The strength of left-eccentric joint model is slightly higher than that of the right-eccentric joint, which is supposed to be resulted from the varying efficiency of protrusion columns. Detailed discussion will be presented in the Section 4.3.

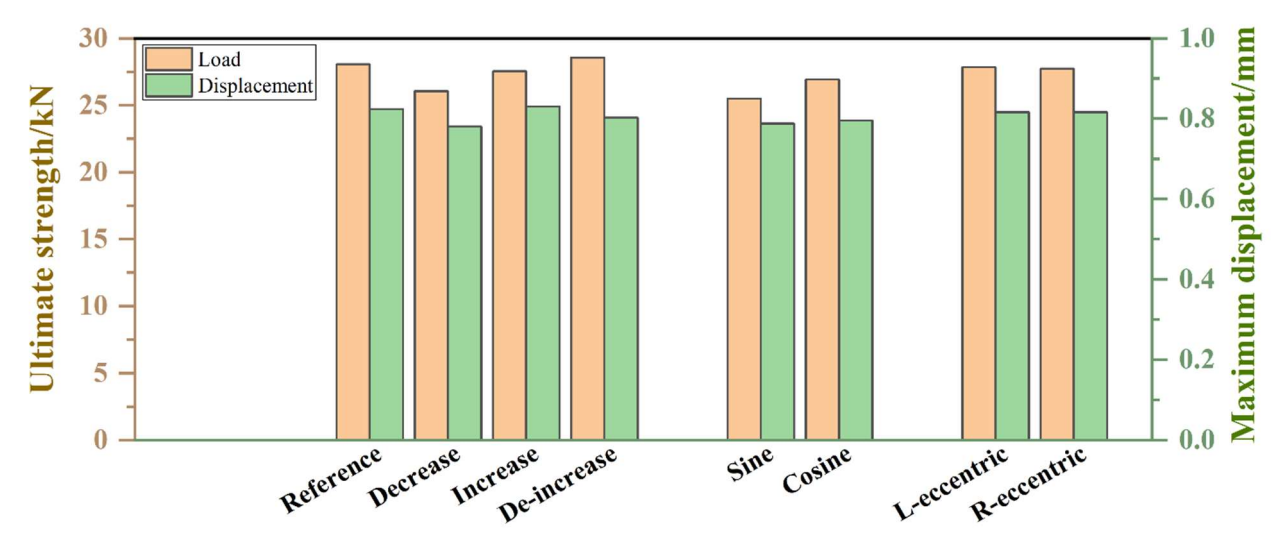


Figure 6 – Ultimate strength and displacement of joints.

#### 4.2 Stress distribution

The Mises stress distribution of different joints under 0.2/0.4/0.6/0.8 mm tensile displacement are illustrated in Figure 7-9. Since the image is drawn on a vertical section, only 9 protrusion columns can be seen. For all of the hybrid joints, the load transferring inside the overlapping area had a similar mode, but the transmission speed and path differed due to the influence of metal protrusions. With the tensile load gradually increasing, the maximum stress point of structure gradually moved from the metal protrusion in left to the composite layer in right.

As shown in Figure 7, although the structural weight is constant, the load-bearing process of these four joints exhibited clearly differences. Losing the obstruction of metal protrusions, stress in the decreasing protrusion height joint directly transferred into the internal area, the protrusions near to the composite end can hardly attached to composite panel, the interface debonding crack extended quickly along the bond line. As a result, the right overlapping area separated early at 0.6 mm tensile displacement, and the entire tensile load were carried by only 2/3 of overlap length, leads to the weakest structural performance of joints. Similar situation was observed in the increasing protrusion height joint, the overlapping area in left exhibited a larger debonding region at 0.8 mm displacement, but the stress had already concentrated in the composite end under this situation, thus had less effect on the joint strength.

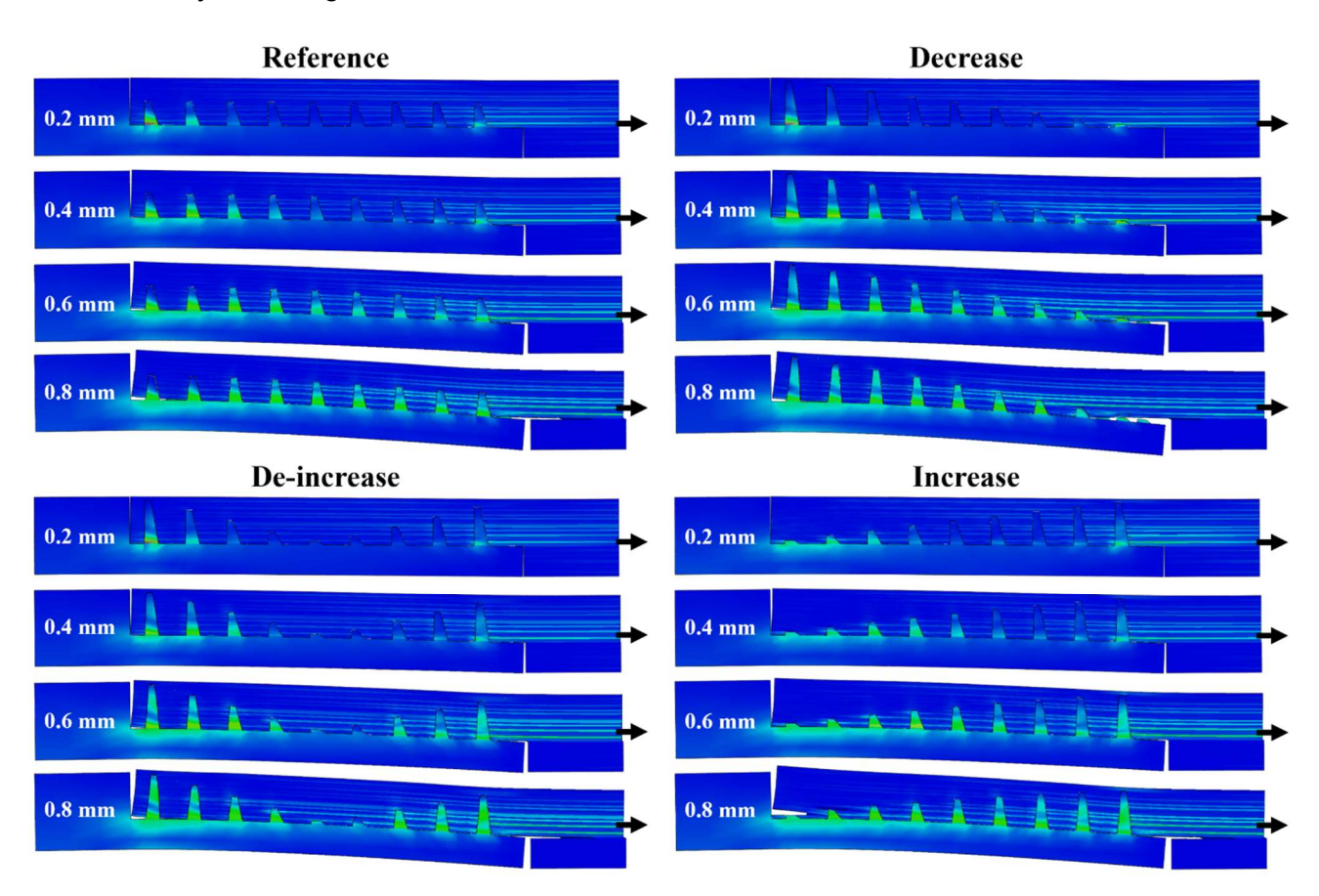


Figure 7 – Stress distribution of monotonically joint models at different tensile displacement. Figure 8 showed the comparison of variable-height hybrid joints with sine and cosine distribution. Apparently, the location of stress concentration area differed in these two models. For the joint with a cosine distribution, the stress mainly concentrated on the composite end, while the stress concentration of joint with sine distribution occurred in a more intermediate position. The tensile load inside the cosine joint was allocated in a dispersed mode. On the contrary, for the sine distributed joint, protrusion columns in the center undertake most of the tensile load, resulted in the movement of stress concentration area. The rotation angle of lap joint became more serious, and the structural stiffness reduced.

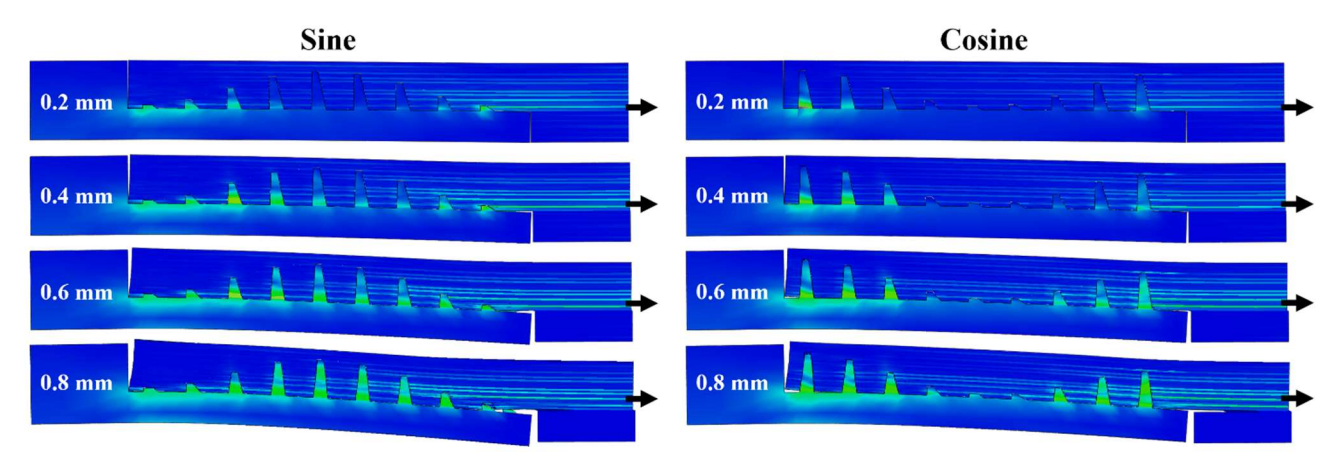


Figure 8 – Stress distribution of sine and cosine joint models at different tensile displacement. As discussed in the former section, the tensile response of two eccentric joints had little difference. This can also be seen from Figure 9, the stress distribution in these two joint models were nearly the same, only the concentration area slightly moved.

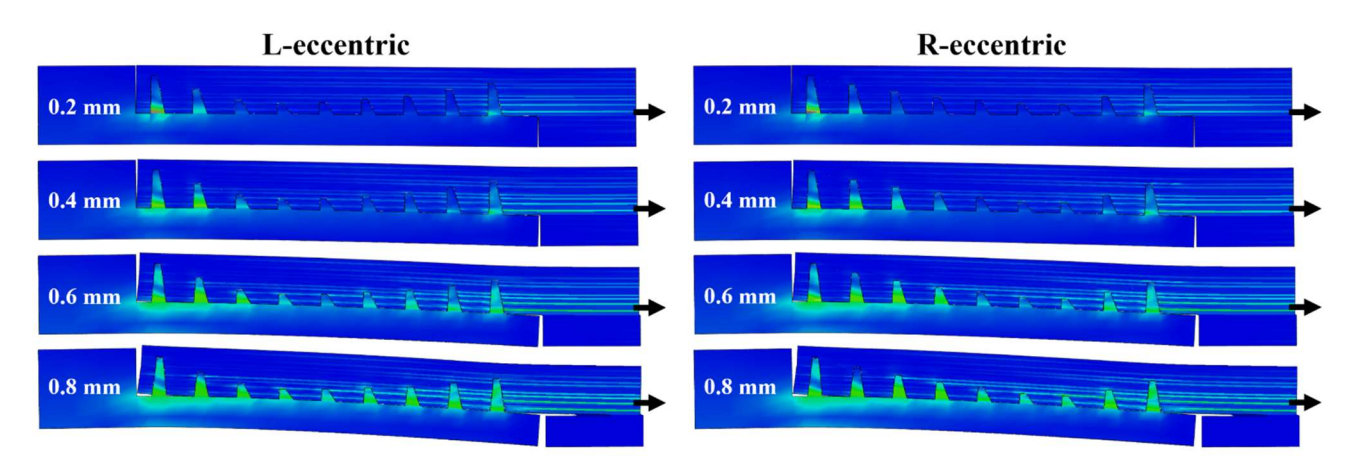


Figure 9 – Stress distribution of eccentric joint models at different tensile displacement.

### 4.3 Deformation of metal protrusions

In order to quantify the loading efficiency of protrusions along bond line, the initiation of plastic strain in each protrusion column was chosen to describe the load-bearing and deformation behavior of metal component. As shown in Figure 2(a) and (b), considering the staggered distribution leads to different numbers of each column and therefore had an effect on the load allocation, metal protrusions located in the odd and even columns are drawn separately. In general, the odd protrusion columns undertake higher stress than the even columns.

Corresponding to the stress transferring process, plastic deformation first occurred in the edge of overlapping area, and then gradually spread into the internal protrusion columns. For the "deincrease" and "cosine" joints, some protrusion columns in the middle area had no plastic deformation until the end of loading procedure. This is because a 0.28 mm protrusion is too weak for load bearing, which can be proved by the stress distribution of each column in Figure 7 and 8. Since the lowest protrusion of 0.84 mm is much stronger to undertake shear stress, these situations did not occur in the eccentric joints. This also explained the prominent points at small X-coordinate, that the plastic deformation in the left column of "increase" and "Sine" joints appeared later than its right side.

The black vertical dashed line in Figure 8-11 represents the central axis of whole overlapping area. It can be clearly seen that the highest point offset from the center, and all of the curves is not symmetrical, especially for the deformation curve of "reference" joint with constant protrusion height. This observation proved that the stress distribution of hybrid lap joint across the X axis is nonuniform, and protrusions in the left side suffered larger plastic deformation than the right side. The phenomenon is supposed to be resulted from the eccentric loading of single lap joint [16] due to its

asymmetric structure.

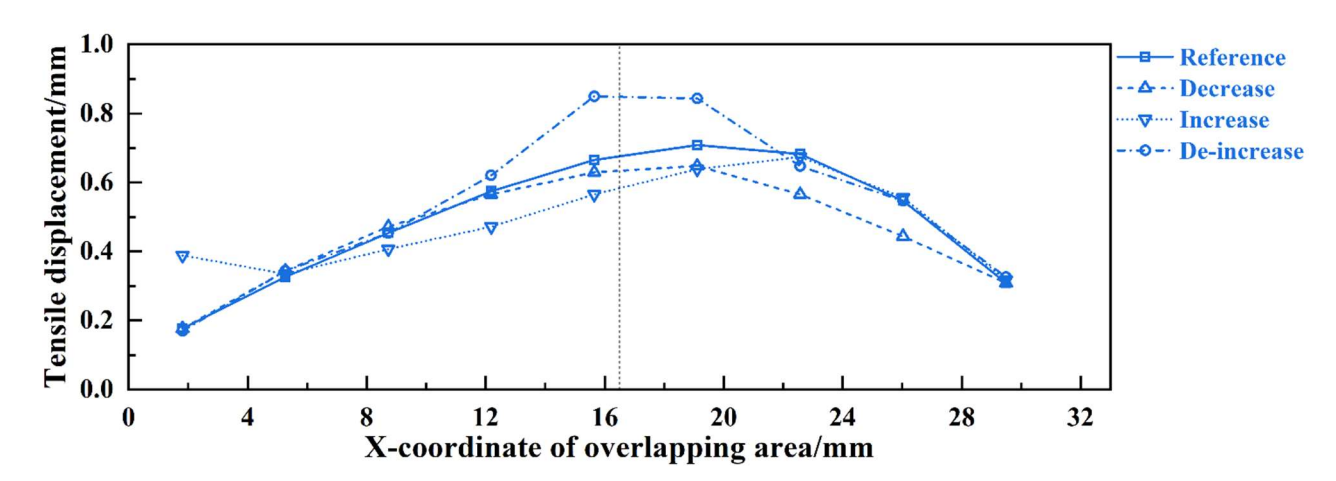


Figure 8 – Initiation of plastic deformation in protrusions of monotonically joints (odd column).

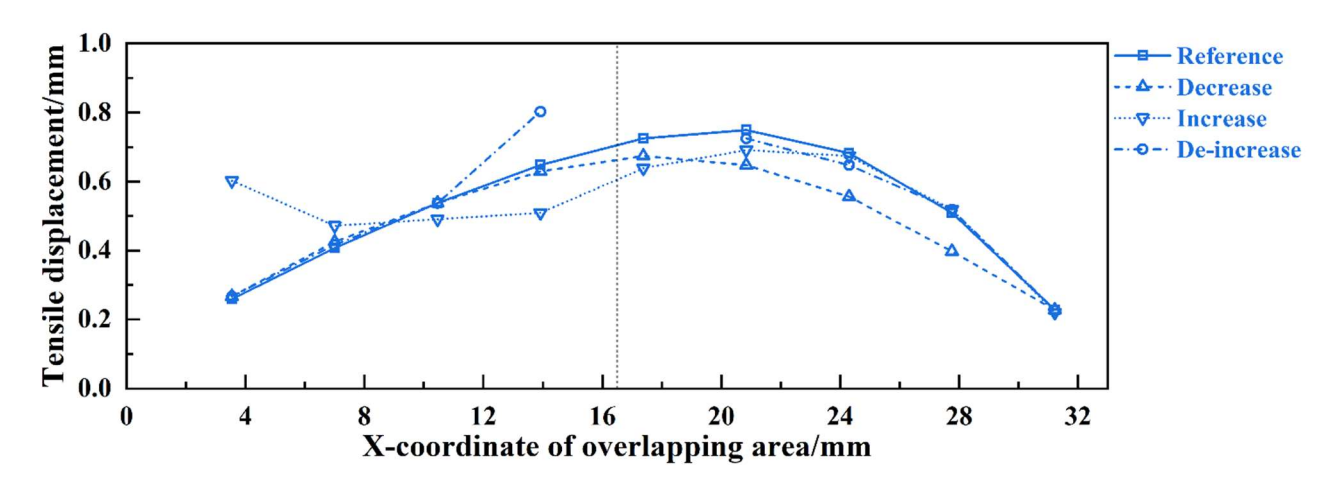


Figure 9 – Initiation of plastic deformation in protrusions of monotonically joints (even column).

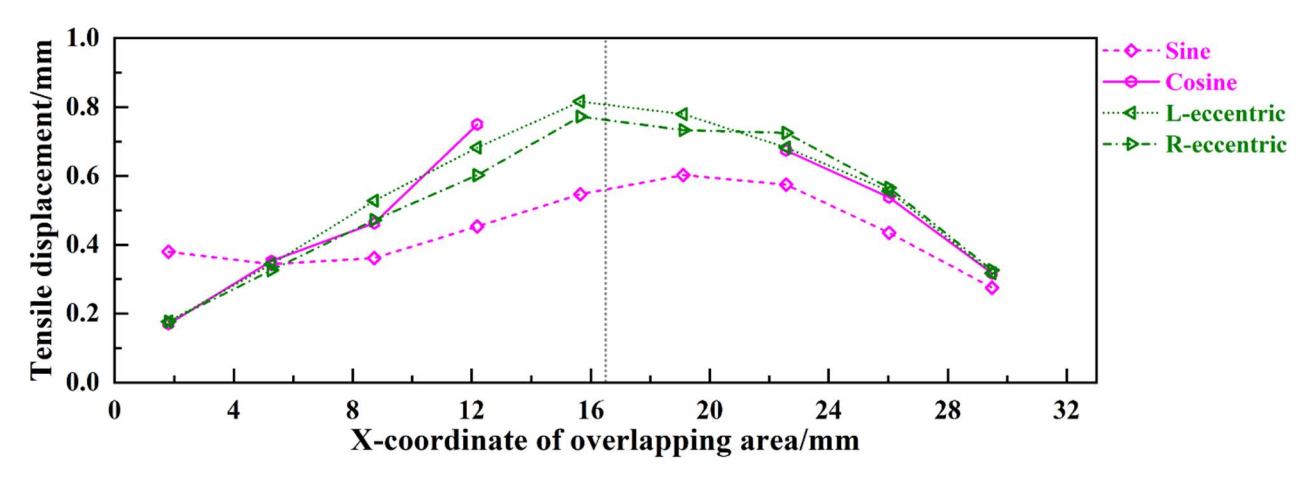


Figure 10 – Initiation of plastic deformation in protrusions of sine/cosine and eccentric joints (odd).

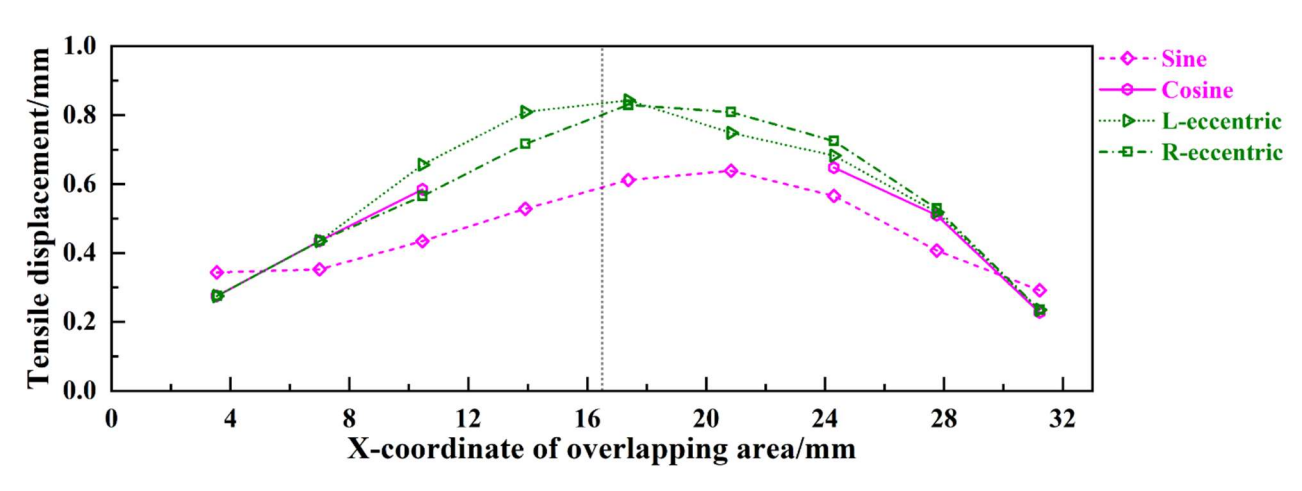


Figure 11 – Initiation of plastic deformation in protrusions of sine/cosine and eccentric joints (even).

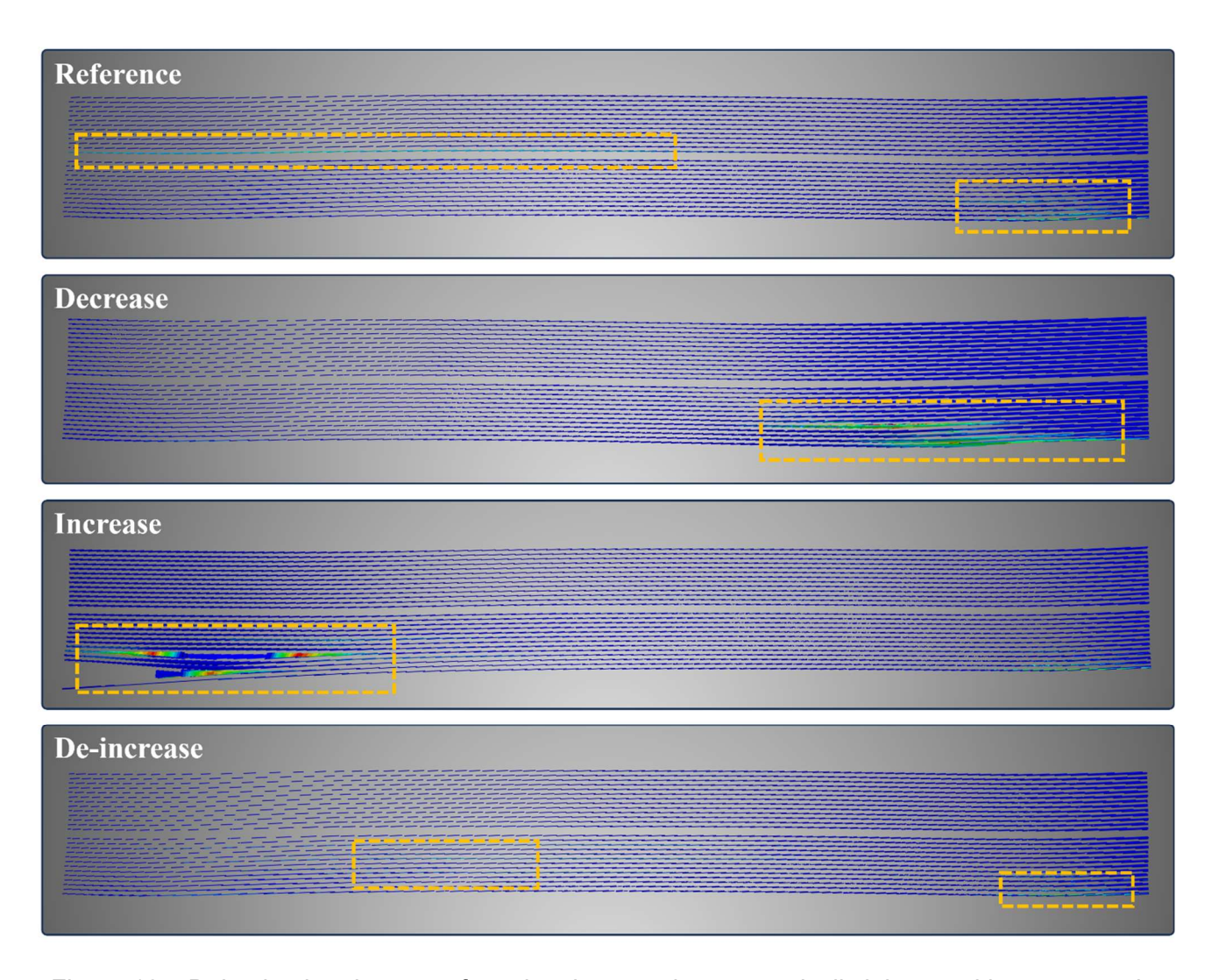


Figure 12 – Delamination damage of overlapping area in monotonically joints at ultimate strength.

# 4.4 Damage of composite panel

As described in Section 2.1, damage variable of the interlayer cohesive elements was used to describe the delamination characteristics of these metal–composite joints. Considering the similar behavior of some joint models and to simplify this paper, only the first group of joints were presented as a representative illustration. For better visual recognition, the images of overlapping area were slightly rotated to be horizontal, as shown in Figure 12. The main region where delamination occurred

in the overlapping area were highlighted by yellow wireframe.

For the reference joint with constant protrusion height, delamination occurred between the layers adjacent to the top of protrusion, and quickly propagated through interlayer when the crack initiated. When the joint structure eventually failed, all of the composite layers underneath the protrusion tip will be separated from the original panel, as shown in Figure 5. Different with the constant height hybrid joint, the application of variable-height protrusion design hindered the propagation of delamination crack. The initial cracks were obstructed by the adjacent column of protrusions with different height. The crack propagation path had to jump to the other layers for further extending, thus can hardly penetrated across the entire plane.

For the joints with monotonically decreasing and increasing protrusion height, the composite delamination only occurred in a limited area with low protrusions reinforced. Compared with the other three models, delamination failure of "de-increase" joint can be hardly detected, and the damaged elements dispersed in more than one layer. These results proved that a rational variable-height protrusion design of hybrid joint can eliminate the risk of delamination.

Despite the suppression of delamination failure inside joint structure, failure analysis conducted on other failure modes of composite (fiber tensile/compression, matrix tensile/compression) showed that the critical failure mode of these joints was all the same. A hybrid joint with medium protrusion numbers always failed after fiber tensile fracture occurred in the composite end. Since the composite fiber is much stronger than the interlaminar elements, the structural strength of hybrid joint is mainly controlled by the fiber tensile strength rather than the interlaminar strength. Therefore, the improvement on ultimate strength was limited by simply altering the distribution of protrusion height. Hopefully, combining the variable-height design with the optimization strategy of other structural parameters can achieve better performance of pin-reinforced hybrid joints.

#### 5. Conclusions

This paper developed a series of metal–composite hybrid joints with variable-height protrusions in ABAQUS<sup>TM</sup>. Based on the finite element method, the loading mechanism and failure behavior of different joints were analyzed. Several conclusions can be drawn from the numerical results:

- (1) The distribution of protrusion height had little effect on the maximum displacement corresponding to ultimate strength, but the structural stiffness changed. The stiffness of hybrid joints with low protrusions at the edges degraded due to the separation of components and the rotation effect.
- (2) Stress distribution in different variable-height joints showed significant differences. The maximum stress point always moved from the metal protrusion to the composite layer, but the load transmission speed varied with the obstruction of protrusion columns. The loading efficiency of protrusion columns near both ends is much higher than that of protrusions in the middle area.
- (3) The plastic strain of each protrusion column was uneven, the ductile damage of metal protrusions on the left side was more severe than on the right side. Plastic deformation of the protrusions located in the 2/3 of overlap length appeared later than in other columns. Protrusions with an excessively low height can hardly bear the structural load.
- (4) Although the variable-height hybrid joints successfully prevented the structure from instantaneous delamination, the ultimate strength of these joints exhibited limited improvement due to the critical failure mode. For joints with low protrusions at the edge of the overlapping area, the load capacity decreased compared with other joints with equal protrusion volume.

In general, a metal—composite joint with high protrusions near the two ends and low protrusions in the middle of the overlapping area exhibits the best joining efficiency. To achieve better mechanical performance and damage tolerance, the design of protrusion height distribution should be combined with other optimized structural parameters, and the non-uniform characteristics of single lap joint can be utilized.

#### 6. Contact Author Email Address

mailto: wangwenzhi@nwpu.edu.cn

# 7. Copyright Statement

The authors confirm that they, and/or their company or organization, hold copyright on all of the original material included in this paper. The authors also confirm that they have obtained permission, from the copyright holder of any third party material included in this paper, to publish it as part of their paper. The authors confirm that they give permission, or have obtained permission from the copyright holder of this paper, for the publication and distribution of this paper as part of the ICAS proceedings or as individual off-prints from the proceedings.

## References

- [1] Shang X, Marques E A S, Machado J J M, Carbas R J C, Jiang D, and Da Silva L F. Review on techniques to improve the strength of adhesive joints with composite adherends. *Composites Part B: Engineering*, Vol. 177, No. 107363, 2019.
- [2] Sarantinos N, Tsantzalis S, Ucsnik S and Kostopoulos V. Review of through-the-thickness reinforced composites in joints. Composite Structures, Vol. 229, No. 111404, 2019.
- [3] Feistauer E E, dos Santos J F, and Amancio Filho S T. A review on direct assembly of through-the-thickness reinforced metal-polymer composite hybrid structures. Polymer Engineering & Science, Vol. 59, No. 4, pp 661-674, 2019.
- [4] Wang X C, Ahn J, Lee J, and Blackman B R K, Investigation on failure modes and mechanical properties of CFRP–Ti6Al4V hybrid joints with different interface patterns using digital image correlation, *Materials & Design*, Vol. 101, pp 188-196, 2010.
- [5] Tu W, Wen P H, Hogg P J and Guild F J. Optimisation of the protrusion geometry in Comeld™ joints. *Composites Science and Technology*, Vol. 71, No. 6, pp 868-876,2011.
- [6] Xiong W, Wang X, Dear J P, and Blackman B R K. The effect of protrusion density on composite-metal joints with surfi-sculpt reinforcement. *Composite Structures*, Vol. 180, pp 457-466,2017.
- [7] Sarantinos N, Kostopoulos V, Di Vita G, Campoli G, and Bricout L. Micro-pins: the next step in composite—composite and metal—composite joining. *CEAS Space Journal*, Vol. 11, pp 351-358,2019.
- [8] Sioutis I, and Tserpes K. A literature review on crack arrest features for composite materials and composite joints with a focus on aerospace applications. *Aerospace*, Vol. 10, No. 2, pp 137,2023.
- [9] Graham D P, Rezai A, Baker D, Smith P A and Watts J F. The development and scalability of a high strength, damage tolerant, hybrid joining scheme for composite–metal structures. *Composites Part A: Applied Science and Manufacturing*, Vol. 64, pp 11-24, 2014.
- [10]Zhao Y R, Zang J, Wan X P, Wang B, Cao Y, Wang W Z, and Chen X M. Failure mechanisms of hybrid metal–composite joints with different protrusion densities under a tensile load. *Mechanics of Advanced Materials and Structures*, pp 1-16, 2023.
- [11] Jiang W G, Hallett S R, Green B G, and Wisnom M R. A concise interface constitutive law for analysis of delamination and splitting in composite materials and its application to scaled notched tensile specimens. *International journal for numerical methods in engineering*, Vol. 69, No. 9, pp 1982-1995, 2007.
- [12] Hashin Z. Failure criteria for unidirectional fiber composites. *Journal of Applied Mechanics*, Vol. 47, No. 2, pp 329-334, 1980.
- [13]Guo W, Xue P, and Yang J. Nonlinear progressive damage model for composite laminates used for low-velocity impact. *Applied Mathematics and Mechanics*, Vol. 34, No. 9, pp 1145-1154,2013.
- [14]Banea M D and da Silva L F. Adhesively bonded joints in composite materials: an overview. *Proceedings of the Institution of Mechanical Engineers, Part L: Journal of Materials: Design and Applications*, Vol. 223, No. 1, 2009.
- [15]Kupski J and De Freitas S T. Design of adhesively bonded lap joints with laminated CFRP adherends: Review, challenges and new opportunities for aerospace structures. *Composite Structures*, Vol. 268, No. 113923,2021
- [16]Ozel A, Yazici B, Akpinar S, Aydin M D, and Temiz Ş. A study on the strength of adhesively bonded joints with different adherends. *Composites Part B: Engineering*, Vol. 62, pp 167-174,2014.